Phase dynamics of coupled oscillators reconstructed from data

Björn Kralemann, Laura Cimponeriu, Michael Rosenblum, and Arkady Pikovsky
Department of Physics and Astronomy, University of Potsdam, Karl-Liebknecht Strasse 24-25, D-14476 Potsdam, Germany

Ralf Mrowka
Institut für Physiologie, AG Systems Biology-Computational Physiology, Charité-Universitätsmedizin Berlin, Berlin, Germany
(Received 29 January 2008; published 9 June 2008)

We systematically develop a technique for reconstructing the phase dynamics equations for coupled oscillators from data. For autonomous oscillators and for two interacting oscillators we demonstrate how phase estimates obtained from general scalar observables can be transformed to genuine phases. This allows us to obtain an invariant description of the phase dynamics in terms of the genuine, observable-independent phases. We discuss the importance of this transformation for characterization of strength and directionality of interaction from bivariate data. Moreover, we demonstrate that natural (autonomous) frequencies of oscillators can be recovered if several observations of coupled systems at different, yet unknown coupling strengths are available. We illustrate our method by several numerical examples and apply it to a human electrocardiogram and to a physical experiment with coupled metronomes.

DOI: 10.1103/PhysRevE.77.066205 PACS number(s): 05.45.Tp, 05.45.Xt, 02.50.Sk, 87.19.Hh

I. INTRODUCTION

Inferring the laws of interaction between different oscillating objects from observations is an important theoretical problem with many experimental applications. Identification and characterization of coupled dynamics from data has been largely approached within the framework of nonlinear dynamics, using techniques developed for bivariate (or, more generally, multivariate) data analysis [1]. In the present work, we concentrate on a revealing phase dynamics description of the interaction of *oscillatory systems*, a highly relevant problem in numerous fields of research: e.g., in the study of coupled lasers [2], electronic systems [3], chemical reactions [4,5], cardiorespiratory interaction [6,7], neuronal systems [8], and functional brain connectivity [9–11], to mention only a few. The major goal of this paper is to show that, under certain assumptions about the intrinsic dynamics and the coupling, it is possible to reconstruct in an observable-independent, invariant way, the equations of the phase dynamics from the observed oscillatory data.

Any technique for reconstructing the phase dynamics equations from data requires as a first step the computation of phase estimates from the observed scalar signals. This computation, based, e.g., on the Hilbert transform, complex wavelet transform, or on the marker event method (see, e.g., [12–14] for details), became a popular tool in the context of a description of the phase synchronization of chaotic oscillators and quantification of synchronization in experiments. As soon as the phases of, say, two interacting oscillators are obtained, one can estimate phase derivatives (instantaneous frequencies) and obtain the desired equations, fitting the dependence of each instantaneous frequency on both phase estimates [15,16]. Reconstructed in this way, the equations capture many important properties of the interaction. For example, these equations can be used for quantification of directionality and delay in coupling [6,16–18], as well as for recovery of the phase resetting curve [8] (see also later publications [5,19]). However, this approach has a fundamental drawback: the phase estimates and reconstructed equations depend on the observables used and, generally, differ from the phases and the equations used in the theoretical treatment of interacting oscillatory systems. To overcome this problem, we propose an approach which bridges the gap between theory and data analysis.

In our approach, we treat the phase estimates, obtained, e.g., via the Hilbert transform, as preliminary variables. To emphasize this issue, we hereafter call these variables *protophases*. Next, we transform the protophases to obtain the observable-independent, genuine phases, which correspond to those used in a theoretical description. In this way, we obtain an *observable-invariant description of the interaction of coupled oscillators.*

We mention two other important features of our approach. First, as an intermediate result we derive a transformation from a protophase to the phase for an autonomous oscillator. This transformation can be used as a preprocessing step for any technique, dealing with phases, e.g., for quantification of the phase diffusion. Second, we develop a technique for recovery of the autonomous frequencies of systems from observations of coupled dynamics. This is possible if two or more observations of the coupled systems for different, though unknown values of the coupling are available.

In this paper we systematically analyze and further develop the approach suggested in our Rapid Communication [20]. The paper is organized as follows. Our approach for reconstructing the phase dynamics is based on the theoretical framework of coupled self-sustained oscillators [12,21], which is briefly outlined in Sec. II. Further, we contrast there the concept of phase used in the theoretical description of autonomous oscillators with that of an angular variable, or protophase, estimated from data. Next, we introduce our approach for the reconstruction of invariant phase dynamics from arbitrary protophases for one oscillator (Sec. III) and for bivariate observations (Sec. IV). In Sec. V, numerical simulation examples are used to validate the efficacy of the proposed methodology. Furthermore, we verify our theory by an experiment with two coupled metronomes—a variant of the classical Huygens study of pendulum clocks (Sec. VI). In

the end (Sec. VII), we discuss the implications of our analysis for characterization and quantification of interaction from data.

II. PRELIMINARIES AND GOALS OF THE WORK

A. Theoretical framework: Coupled oscillators in the phase approximation

Let us recall basic notions of the phase dynamics. Mathematically, an autonomous oscillator is described by a vector of state variables $\mathbf{x}$ and a differential equation of motion, $\dot{\mathbf{x}}=\mathcal{F}(\mathbf{x})$. When such a system has a stable limit-cycle solution $\mathbf{x}_0(t)=\mathbf{x}_0(t+T_0)$, then the motion on the limit cycle and in its vicinity can be characterized by a phase $\phi(\mathbf{x})$, which grows linearly with time according to

$$\dot{\phi}=\omega_0, \tag{1}$$

where $\omega_0=2\pi T_0^{-1}$ is the natural (autonomous) frequency [12,21]. A perturbation (say, periodic or noisy) to the pure autonomous equation leads to a deviation of the phase ϕ from the linear growth (1), resulting in such effects as phase locking or phase diffusion.

Of particular interest is the description of the interaction of two oscillators in terms of their phases. As the first step of the theoretical treatment, one introduces phases $\phi_{1,2}$ for two uncoupled autonomous systems; these phases grow with natural frequencies $\omega_{1,2}$. Next, the coupling terms in the governing equations should be taken into account. (In a more complex setting, the coupling may include additional dynamical variables requiring additional equations.) Physically, the coupling appears, e.g., due to an overlap of radiation fields of two lasers or due to synaptic and/or gap junction currents between interacting neurons, etc. For the following it is convenient to distinguish between weak, moderate, and strong coupling.

If the coupling is weak, the dynamics of the coupled system is confined to a torus in the phase space; hence, it can effectively be described by means of two phases only. This description can be obtained explicitly with the help of a perturbation technique, where one neglects the dynamics of the amplitudes, because they are robust. The robustness of the amplitude follows from the fact that the amplitude corresponds to the direction in the phase space, transversal to the limit cycle, and this direction is stable. Its stability is characterized by the negative Lyapunov exponent λ_- of the dynamical system. Hence, the amplitude can be considered as enslaved if the magnitude of forcing or coupling is much less than $|\lambda_-|$. Contrary to the amplitude, the phase corresponds to the direction along the limit cycle and, correspondingly, to the zero Lyapunov exponent. Thus, the phase is a marginally stable variable and is therefore affected even by a weak external perturbation, which can be due to coupling or due to noise; see [12,21] for more details. The result of the application of the perturbation technique is the following system of equations:

$$\dot{\phi}_1=\omega_1+q^{(1)}(\phi_1,\phi_2),$$

$$\dot{\phi}_2=\omega_2+q^{(2)}(\phi_2,\phi_1), \tag{2}$$

where $q^{(1,2)}$ are coupling functions which are 2π periodic with respect to their arguments. Due to coupling, the averaged velocities of phase rotation,

$$\Omega_1=\langle\dot{\phi}_1(t)\rangle, \quad \Omega_2=\langle\dot{\phi}_2(t)\rangle, \tag{3}$$

called observed frequencies, generally differ from $\omega_{1,2}$. Solutions of the system (2) can be quasiperiodic, with incommensurate $\Omega_{1,2}$, or periodic. The latter case is designated as synchronization.

In the case of moderate coupling, the approximation used in the perturbation theory is not valid anymore, so that Eqs. (2) cannot be explicitly derived from the equations in state variables. However, the equations in this form still exist. Indeed, as long as the full dynamics remains confined to the torus, it still can be described by two phase variables. Finally, a strong coupling means that the torus is destroyed, e.g., due to the emergence of chaos and Eqs. (2) are not valid anymore.

Real-world systems are unavoidably noisy. However, when the noise is weak, it can be accounted for by incorporating random terms into Eqs. (2), so that Eqs. (2) become Langevin-type equations. These equations have been also suggested for describing the dynamics of weakly coupled chaotic oscillators [12].

For the rest of the paper we restrict our consideration to the case of weakly and moderately coupled noisy-chaotic oscillatory systems in the asynchronous regime—i.e., to the case when the amplitudes are enslaved and the phase portrait of the individual system resembles a smeared limit cycle. In this case, the coupled system can be adequately described by the phase variables.

B. Phases vs protophases

In the theoretical consideration of a particular periodic oscillatory system, an analytical expression for the phase $\phi(\mathbf{x})$ obeying Eq. (1) can be found only in exceptional cases. As the first step, one typically introduces an angle variable on the cycle, or protophase, $\theta=\theta(\mathbf{x}_0)$, which grows monotonically within one oscillation period T_0 and obeys $\theta(\mathbf{x}_0(t+T_0))=\theta(\mathbf{x}_0(t))+2\pi$. This can be easily done numerically once the dynamical equations are known. For example, in many cases θ can be identified with an angle $\theta=\arctan y_2/y_1$ in a projection of the limit cycle onto some plane (y_1,y_2). Obviously, the choice of the protophase θ is not unique: different projections generally yield different protophases. However, it does not constitute a problem, since any protophase $\theta(\mathbf{x}_0(t))$ can be easily transformed to the unique phase $\phi(\mathbf{x}_0(t))$. Indeed, from

$$\frac{d\phi}{dt}=\frac{d\phi}{d\theta}\frac{d\theta}{dt}=\omega_0,$$

we obtain

$$\frac{d\phi}{d\theta} = \frac{\omega_0}{\frac{d\theta}{dt}(\theta)} = \omega_0 \frac{dt}{d\theta}(\theta), \tag{4}$$

which further reveals the desired transformation

$$\phi = \omega_0 \int_0^\theta \frac{dt}{d\theta}(\theta')d\theta'. \tag{5}$$

[We impose an additional condition $\phi(\theta=0)=0$.]

The crucial issue raised by our study is that the *above discussed distinction between protophases and phases has never been exploited in the context of data analysis*. Indeed, all known methods of phase estimation from data (see [12–14] and detailed discussion below)—e.g., via the Hilbert transform—actually provide protophases which heavily depend on the scalar observables available and on the analysis technique. If the goal of the analysis is the quantification of the frequency locking, then the difference between phases and protophases is not relevant, since they provide the same average frequencies, $\langle\dot{\phi}\rangle=\langle\dot{\theta}\rangle$. However, if the goal of the analysis is to get more insight into the interaction and to reconstruct the equations of the phase dynamics, this difference becomes decisive. Indeed, in terms of protophases Eqs. (2) read

$$\dot{\theta}_1 = f^{(1)}(\theta_1, \theta_2),$$

$$\dot{\theta}_2 = f^{(2)}(\theta_2, \theta_1), \tag{6}$$

where the functions $f^{(1,2)}$ depend on the choice of protophases $\theta_{1,2}$. Equations (6) can be easily reconstructed from the data (see [16] and Sec. IV A below), but they do not provide a complete, invariant description of interaction, since they are observable dependent.

The main goal of our study is to develop a technique for transformation of protophases to true phases, $\theta_{1,2}\to\phi_{1,2}$, and for a subsequent transformation of observable-dependent functions $f^{(1,2)}$ to observable-invariant coupling functions $q^{(1,2)}$. Next, we propose a solution for the problem of the determination of autonomous frequencies $\omega_{1,2}$ from observations of coupled systems. Note that the latter task is highly nontrivial: the functions $f^{(1,2)}$ can be represented as a Fourier series, but their constant terms do not equal $\omega_{1,2}$. Before addressing the problem of two coupled oscillators, we first discuss how the transformation (5) can be extended to treat the case of a noisy or a weakly chaotic autonomous oscillator.

III. ONE OSCILLATOR: FROM TIME SERIES TO PHASE

In this section we describe our approach for recovering the phase of an autonomous oscillator from a single oscillating scalar observable. This case, being interesting by itself, is a necessary first step for the subsequent consideration of multivariate data.

A. From time series to protophase

The first step of data analysis is to obtain a protophase $\Theta(t)$ from an oscillatory scalar time series $Y(t)$; the latter is assumed to be generated by a noisy or a weakly chaotic self-sustained oscillator. (In the following we denote the time series of corresponding observables by capital letters.) Note that observable $y(t)$ is generally a nonlinear function of state variables $\mathbf{x}$; we require it to be nondegenerate.

There are different ways to accomplish this task. The most popular approach is to construct the analytic signal $s(t)=Y(t)+i\hat{Y}(t)$, where $\hat{Y}(t)$ is the Hilbert transform of $Y(t)$ [22]; see also [12] for details of practical implementation. For an oscillatory signal $Y(t)$, the Hilbert transform provides a two-dimensional embedding of the (smeared) limit cycle or strange attractor. A protophase Θ can be computed by taking the argument of $s(t)$,

$$\Theta(t) = \arctan\left(\frac{\hat{Y}(t)-\hat{Y}_0}{Y(t)-Y_0}\right), \tag{7}$$

and then unwrapping it so that it is defined on a real line. Here $(Y_0,\hat{Y}_0)$ is an offset point, chosen in such a way that it is evolved by the trajectory. Alternatively, one can exploit the complex wavelet transform [13,14], which is equivalent to a subsequent application of a bandpass filter and the Hilbert transform [31]. Obviously, the protophase obtained according to (7) depends not only on the observable Y, but also on the offset $(Y_0,\hat{Y}_0)$.

As already mentioned, to obtain the phase ϕ by means of a transformation $\theta\to\phi$ we need a protophase that grows monotonically within one oscillatory cycle. However, if the protophase is chosen according to Eq. (7), monotonicity is not ensured. For example, θ is not monotonic if the trajectory in the embedding $(y,\hat{y})$ intersects itself [cf. Figs 1(a) and 1(d) below]. However, in this case, we can define a monotonic protophase in a following way. First, we choose a Poincaré surface of section and denote the moments of time when the trajectory intersects this surface as t_i. Next, we compute the length $L(t)$ along the trajectory, starting from the first intersection. The protophase is then defined as

$$\Theta(t) = 2\pi\frac{L(t)-L(t_i)}{L(t_{i+1})-L(t_i)} + 2\pi i, \quad t_i < t < t_{i+1}. \tag{8}$$

This definition can be considered as a generalization of the marker event method [12]. Note that using the marker event protophase—i.e., linearly interpolating phase between two intersections with the Poincaré surface of section—we lose the information about the fast (of the order of the oscillation period) component of the phase dynamics and retain only information about the slow variation of the phases. Hence, although this technique is useful, e.g., for the computation of observed frequencies, is of a limited use if a complete reconstruction of the phase dynamics is required. This issue, as well as a determination of protophases from observables of different complexity, will be discussed elsewhere [23].

Note that in the following we alternatively, depending on the context, use both wrapped (defined on $0,2\pi$ interval) and unwrapped (defined on the real line) phases and protophases.

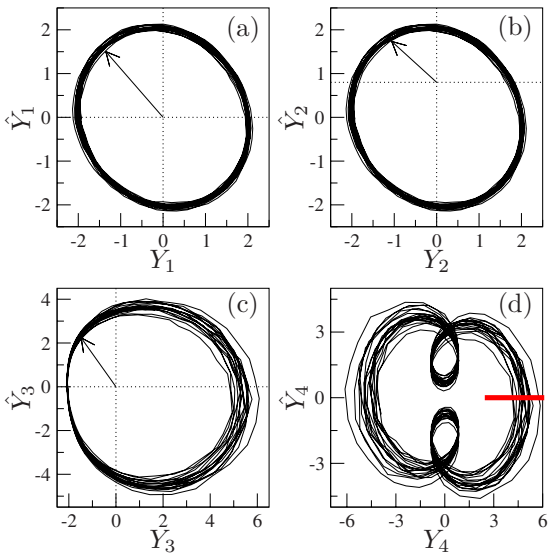

FIG. 1. (Color online) Embedding of data from the van der Pol oscillator [Eq. (17)] in coordinates Y_i and $\hat{Y}_i$, where $\hat{Y}_i$ is the Hilbert transform of Y_i, for four different observables (see text). In (a), (b), and (c) the protophases have been obtained according to Eq. (7), as corresponding angles. In (d) the protophase has been obtained via the length of the trajectory according to Eq. (8). The bold red line in (d) marks the Poincaré section used for this computation.

B. From protophase to phase

Once a monotonic protophase $\theta(t)$ has been obtained from a time series, we can look for a transformation $\theta(t) \to \phi(t)$. For a noise-free limit-cycle oscillator this transformation is given by Eq. (5). Our next goal is to extend this transformation to the case of a noisy system. The sought transformation shall satisfy two requirements: (i) it should be 2π periodic in θ and (ii) it should minimize the deviations of ϕ from the linear growth—i.e., provide a maximally uniform instantaneous frequency $\dot{\phi}$.

In the presence of weak noise and/or chaos, the state trajectory does not repeat itself. However, for small perturbations, the trajectory of the stable oscillator is expected to remain close to the unperturbed one. In this case, the transformation $\theta \to \phi$ can be performed on average, requiring a sufficiently long observation of the oscillatory time series. Given an estimated protophase $\Theta(t)$ over a time interval T, the oscillation frequency can be computed from

$$\omega_0 = \frac{\Theta(T) - \Theta(0)}{T}.$$

To find the desired transformation, we average the right-hand side (rhs) of (4) and write

$$\frac{d\phi}{d\theta} = \omega_0 \left\langle \frac{dt}{d\theta}(\theta) \right\rangle_\theta = \sigma(\theta), \tag{9}$$

where, in $\langle \cdots \rangle$, the average is taken over all the oscillation cycles. Alternatively, due to ergodicity, the average over θ can be replaced by time integration over the trajectory:

$$\langle (\cdots) \rangle = \frac{1}{T} \int_0^T (\cdots) dt. \tag{10}$$

The function $(2\pi)^{-1}\sigma(\theta)$ is nothing else but the probability distribution density of θ, as it is inversely proportional to the velocity of the point on the trajectory. The probability density can be written as

$$(2\pi)^{-1}\sigma(\theta) = \langle \delta(\Theta(t) - \theta) \rangle, \tag{11}$$

where the average is taken in the sense of Eq. (10).

Let us represent $\sigma(\theta)$ as a Fourier series

$$\sigma(\theta) = \sum_n S_n e^{in\theta}, \tag{12}$$

with the coefficients

$$S_n = \frac{1}{2\pi} \int_0^{2\pi} \sigma(\theta) e^{-in\theta} d\theta. \tag{13}$$

The term $S_0 = 1$ ensures the normalization condition for the probability density. Substituting (11) into (13), we obtain

$$S_n = \frac{1}{T} \int_0^T dt \int_0^{2\pi} d\theta \, e^{-in\theta} \delta(\Theta(t) - \theta) = \frac{1}{T} \int_0^T e^{-in\Theta(t)} dt. \tag{14}$$

For a time series given as N_p points $\Theta(t_j)$ sampled with time step T/N_p, where $t_j = jTN_p^{-1}$, we replace the integration by summation and obtain

$$S_n = \frac{1}{N_p} \sum_{j=1}^{N_p} e^{-in\Theta(t_j)}. \tag{15}$$

Finally, using Eqs. (9) and (12), we obtain the desired transformation in the form

$$\phi = \int_0^\theta \sigma(\theta') d\theta' = \sum_n S_n \int_0^\theta e^{in\theta'} d\theta' = \theta + \sum_{n \neq 0} \frac{S_n}{in} (e^{in\theta} - 1). \tag{16}$$

Equations (14)–(16) solve the problem of finding the transformation from a protophase to the phase. Transformation (16) gives the perfectly linearly growing phase for periodic noiseless oscillations. For a time series with noise it gives the best possible approximation to the linearly growing phase, where all nonuniformities, 2π periodic in the protophase, are eliminated and deviations of $\phi(t)$ from a strictly linear growth account only for external influences or fluctuations of the parameters of the underlying dynamical system.

C. Numerical example

We illustrate our theoretical consideration by simulation of a noisy van der Pol oscillator described by

$$\ddot{x} - \mu(1 - x^2)\dot{x} + \omega^2 x = 0.05\xi(t), \tag{17}$$

where $\mu = 0.5$, $\omega = 1.11$, and $\xi(t)$ denotes δ-correlated Gaussian noise. We solve the system numerically using the Euler method and estimate the protophase using four different observables.

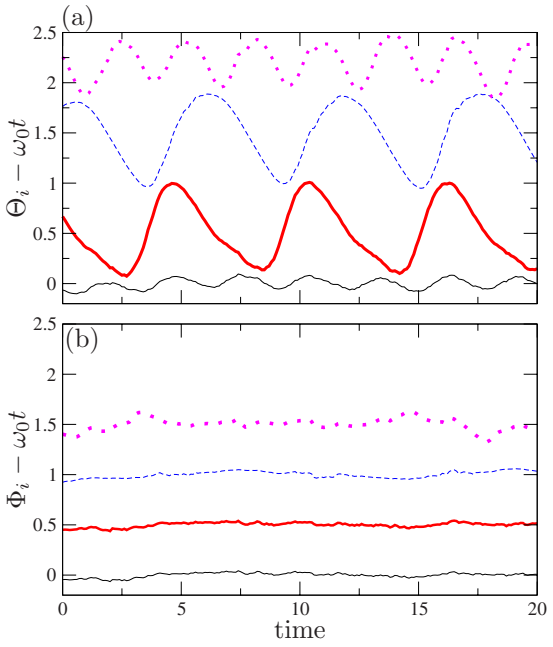

FIG. 2. (Color online) Deviation of the angle variables Θ_i (a) and phases Φ_i (b) from linear growth for four different observables of the van der Pol system (see text) are shown by solid black line, red bold line, dashed blue line, and dotted magenta line, respectively (the lines are vertically shifted for clarity of presentation). It is clearly seen that the transformation $\theta \to \phi$ makes the growth of the corresponding variable almost uniform. Note that the bold red and solid black lines in (b) practically coincide; it means that our transformation $\theta \to \phi$ completely removes the effect of the linear shift of the reference point for the angle calculations [cf. Figs 1(a) and 1(b)].

(i) The first observable is just the solution of Eq. (17)—i.e., $Y_1(t)=x(t)$—and the first protophase Θ_1 is computed according to Eq. (7) with $Y_0=\hat{Y}_0=0$.

(ii) The second protophase Θ_2 is obtained from $Y_2(t)=x(t)$ with $Y_0=0$, $\hat{Y}_0=0.8$.

(iii) The third observable is obtained via a monotonic nonlinear transformation of $x(t)$: $Y_3(t)=\exp[x(t)]-2.2$; $Y_0=\hat{Y}_0=0$.

(iv) Finally, the fourth observable is obtained via a nonmonotonic transformation: $Y_4(t)=[x^2(t)-1.7]x(t)$; $Y_0=\hat{Y}_0=0$.

The phase portraits of the system in coordinates $Y_i, \hat{Y}_i$ are shown in Fig. 1. Obviously, in cases (i), (ii), and (iii) [Figs. 1(a)–1(c)], rotation of the phase point is monotonic, so that we can estimate protophases $\Theta_{1,2,3}(t)$ according to Eq. (7). For estimation of $\Theta_4(t)$ [Fig. 1(d)] we employed the approach based on the length of the trajectory [Eq. (8)]; the Poincaré section used for this procedure is shown by the bold red line in Fig. 1(d). The deviations of the obtained phase estimates Θ_i, $i=1,\ldots,4$ from the linear growth $\omega_0 t$ are shown in Fig. 2(a).

Next, we compute from these estimates the phases Φ_i, according to Eqs. (15) and (16) using 48 Fourier terms in expansion (16); the results are shown in Fig. 2(b). One can see that for all observables the deviation from a linear growth is drastically reduced by the transformation $\theta \to \phi$. However,

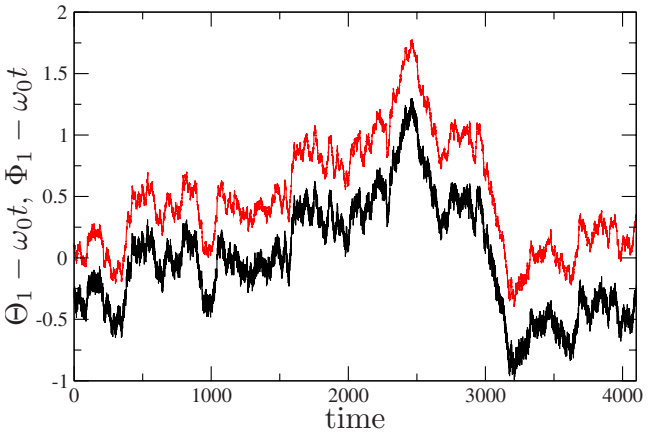

FIG. 3. (Color online) The phase diffusion in the noisy van der Pol oscillator (17) is preserved by the transformation (16), as illustrated by the protophase Θ_1 and phase Φ_1, obtained from the first observable (see text). The curve for the phase is shifted up for presentation purposes.

as we illustrate in Fig. 3, our transformation preserves long-time-scale features of the phase dynamics: e.g., the phase diffusion. Moreover, we stress that the *transformation (16) is fully invertible* and does not mean any "filtering" of the data. Another way to illustrate the effect of the transformation is to compare the distributions of wrapped protophases and correspondent phases (Fig. 4). Summarizing this example, we conclude that our method efficiently works with simulated data of the noisy self-sustained oscillator considered here.

D. Experimental data: Three ECG lead measurements

For the second example we estimate the protophases Θ and phases Φ from three-channel electrocardiogram (ECG) measurements from a healthy male. The data are taken from the *PhysioNet* database [24] (subject *mgh001* of database *MGH/MF*). Hence, we have at our disposal three different observations of the same oscillatory system. The sampling frequency used by the recording system was 1 kHz. The Hilbert plane representations of these channels are presented in Fig. 5. It can be seen that a monotonic protophase cannot be obtained according to Eq. (7) due to the fact that the trajectories are folded and display small loops, smeared by

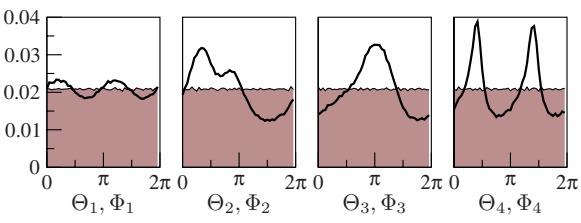

FIG. 4. (Color online) The probability density of protophases $\Theta_i(\mathrm{mod}\ 2\pi)$ (bold curves) and of the phases $\Phi_i(\mathrm{mod}\ 2\pi)$ (solid regions), obtained from different observables of the van der Pol oscillator. While the distributions of the phase estimates $\Theta_i(t)$ are not uniform and depend on the observables, the transformed, genuine phases of all observables are practically uniformly distributed.

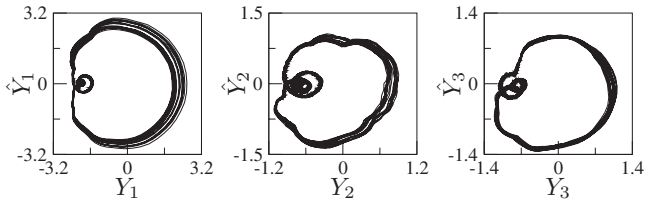

FIG. 5. Three channels of a multiple-lead ECG measurement, represented in $Y_i, \hat{Y}_i$ coordinates, where $\hat{Y}_i$ is the Hilbert transform of Y_i.

noise. Hence, we estimate the angular variables with the help of Eq. (8).

The protophases and the phases obtained with the help of transformation (16) for all channels are shown in Figs. 6(a) and 6(b), respectively [200 Fourier terms have been used in the transformation (15) and (16)]. Noteworthy, the phases $\Phi_{1,2,3}(t)$ computed from three different observables nearly coincide and exhibit a similar slow deviation from a linear growth. These deviations can be attributed to external perturbations to the cardiovascular system, most likely due to respiratory-related influences. Figure 7 illustrates the effect of the transformation $\Theta_i \to \Phi_i$ on the distributions of $\Theta_i(\mathrm{mod}\ 2\pi)$ and $\Phi_i(\mathrm{mod}\ 2\pi)$. As expected, the distributions of the phases Φ are nearly uniform.

Figure 6(c) shows the evolution of the phase during a longer time interval. Here the deviations from a uniform growth become apparent, and one recognizes two characteristic time scales of these deviations: (i) a shorter time scale,

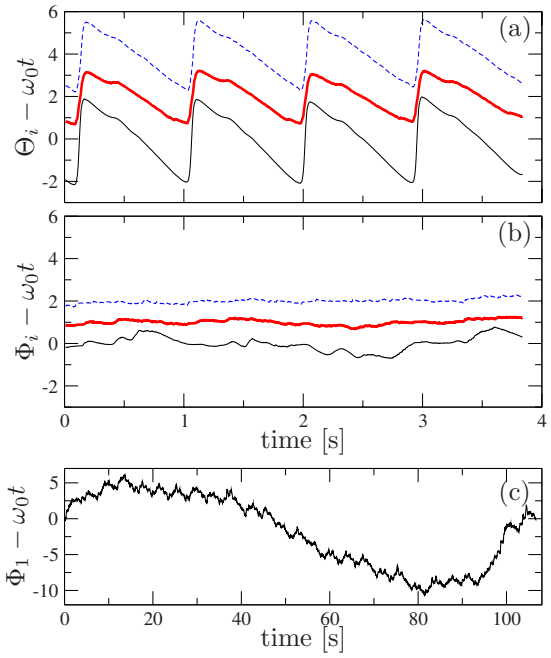

FIG. 6. (Color online) Protophases (a) Θ_i and phases (b) Φ_i of three ECG channels. (The curves are vertically shifted for presentation purposes.) Panel (c) shows Φ_1 on a large time scale. One can see that our transformation preserves all the low-frequency features, including the phase diffusion. In particular, one can see a regular modulation of the cardiac phase with period ≈ 4 s, which is most likely due to influence of respiration.

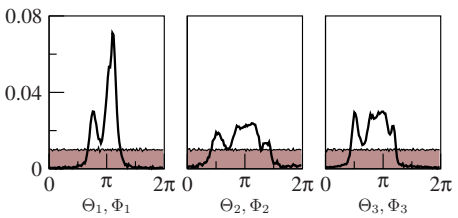

FIG. 7. (Color online) The distributions of phase estimates $\Theta_i(\mathrm{mod}\ 2\pi)$ (bold lines) and of the phases $\Phi_i(\mathrm{mod}\ 2\pi)$ (solid regions), obtained from three ECG channels.

of about ≈ 4 s, corresponding presumably to respiratory influences, and (ii) slower variations with time scale ≈ 1 min. Hence, cleaning away inhomogeneities at the time scale of one oscillatory period (≈ 1 s), the transformation to the phase preserves the manifestation of external perturbations to the heart rhythm, thus providing an opportunity for an efficient analysis of these perturbations. Important is that the resulting time series of the phase is practically independent of the observable used (i.e., of the ECG channel).

At the end of this discussion we would like to mention that using the phases obtained from different channels with uncorrelated measurement noise one can reduce this noise by averaging over observables; all noisy components which are common for different measurements remain, of course, preserved.

IV. FROM BIVARIATE TIME SERIES TO PHASE DYNAMICS EQUATIONS

In this section we describe how the phases $\phi_{1,2}$, as well as the equations for their dynamics, Eqs. (2), can be reconstructed from the observations of two scalar observables $y_{1,2}$. A generalization of our approach to the case of a larger number of interacting oscillators will be discussed elsewhere [23]. The first step—obtaining the protophases $\Theta_{1,2}(t)$ from the time series $Y_{1,2}(t)$—was described in Sec. III A above; thus, now we presume that time series of protophases $\Theta_1(t)$, $\Theta_2(t)$, $0 \le t \le T$, are already available.

A. From time series to equations for protophases

We assume that the protophases stem from coupled oscillators satisfying Eq. (6), and we try to reconstruct these equations. The first observation is that this is possible only in the nonsynchronous case when the oscillations are quasiperiodic or nearly quasiperiodic (as we presume that the data are noisy, the exact notion of quasiperiodicity does not apply). Indeed, in the case of synchrony (for simplicity we can consider 1:1 locking) one observes a periodic motion with a certain relation between the phases; i.e., the observables $\Theta_{1,2}$ are functionally related. Therefore it is impossible to reconstruct functions of two variables in (6), because these functions are observed not on the full torus $0 \le \Theta_{1,2} < 2\pi$, but only on a line. On the other hand, in the absence of synchrony, when the observed regime is nonperiodic, there is no relation between the observed protophases $\Theta_{1,2}$ and one may hope to reconstruct the functions of two variables in (6). It is clear, that this reconstruction will work better if the angles

nearly uniformly cover the torus $0 \leq \Theta_{1,2} < 2\pi$.

The next step is the estimation of the rhs of (6). For simplicity of presentation we consider only the first equation to be reconstructed:

$$\dot{\Theta}_1(\theta_1,\theta_2) = f^{(1)}(\theta_1,\theta_2) = \sum_{n,m} F^{(1)}_{n,m} e^{in\theta_1+im\theta_2}. \tag{18}$$

We find the coupling function by minimizing the error of approximation in (18) according to

$$\left\langle \left(\dot{\Theta}_1 - \sum_{n,m} F^{(1)}_{n,m} e^{in\theta_1+im\theta_2}\right)^2 \right\rangle = \int_0^{2\pi}\int_0^{2\pi} d\theta_1 d\theta_2 \rho(\theta_1,\theta_2) \times \left(\dot{\Theta}_1 - \sum_{n,m} F^{(1)}_{n,m} e^{in\theta_1+im\theta_2}\right)^2 \stackrel{!}{=} \min, \tag{19}$$

where $\rho(\theta_1,\theta_2)$ is the probability density. The minimization condition leads to a linear system

$$\int_0^{2\pi}\int_0^{2\pi} d\theta_1 d\theta_2 \rho(\theta_1,\theta_2) e^{in\theta_1+im\theta_2} = \sum_{k,l} F^{(1)}_{kl} \int_0^{2\pi}\int_0^{2\pi} d\theta_1 d\theta_2 \rho(\theta_1,\theta_2) e^{i(n+k)\theta_1+i(m+l)\theta_2}. \tag{20}$$

Replacing the integration over θ_1,θ_2 through the integration over the time according to

$$\langle(\cdots)\rangle = \int_0^{2\pi}\int_0^{2\pi} \rho(\theta_1,\theta_2)(\cdots) d\theta_1 d\theta_2 \to \frac{1}{T}\int_0^T (\cdots) dt \tag{21}$$

[this expression is analogous to Eq. (10)], we can rewrite this system as

$$\sum_{k,l} A_{n+k,m+l} F^{(1)}_{kl} = B_{n,m}, \tag{22}$$

where

$$A_{n+k,m+l} = \frac{1}{T}\int_0^T dt\, e^{i(n+k)\Theta_1(t)+i(m+l)\Theta_2(t)}, \tag{23}$$

$$B_{n,m} = \frac{1}{T}\int_0^{\Theta_1(T)} d\Theta_1 e^{in\Theta_1+im\Theta_2}. \tag{24}$$

Similar to Eq. (15), we can also write Eqs. (23) and (24) as sums over the discrete time series:

$$A_{n+k,m+l} = \frac{1}{N_p}\sum_{j=1}^{N_p} e^{i(n+k)\Theta_1(t_j)+i(m+l)\Theta_2(t_j)}, \tag{25}$$

$$B_{n,m} = \frac{1}{N_p-2}\sum_{j=2}^{N_p-1} \frac{\Theta_1(t_{j+1})-\Theta_1(t_{j-1})}{2} e^{in\Theta_1(t_j)+im\Theta_2(t_j)}. \tag{26}$$

For the second protophase θ_2, the corresponding equations read

$$\sum_{k,l} A_{n+k,m+l} F^{(2)}_{kl} = C_{n,m}, \tag{27}$$

where

$$C_{n,m} = \frac{1}{T}\int_0^{\Theta_2(T)} d\Theta_2 e^{in\Theta_1+im\Theta_2}. \tag{28}$$

These formulas solve the problem of finding the coupling functions $f^{(1,2)}$ in Eq. (6) from the linear equations (22) and (27).

B. From protophases to phases

Now we want to find a transformation from the protophases satisfying Eq. (6) to phases $\phi_{1,2}$, which satisfy Eq. (2). We immediately see that this condition is not well defined, as in system (2) we have a clear separation between terms of the coupling $q^{(1,2)}$ and the natural frequencies $\omega_{1,2}$ only if the latter are known. Otherwise, this separation is ambiguous, because coupling functions $q^{(1,2)}$ generally contain constant terms. Therefore, here we have to make an additional assumption: *we assume that the coupling terms* "oscillatory" *depend on the forcing phase.* This means that the following conditions are valid:

$$\int_0^{2\pi} q^{(1)}(\phi_1,\phi_2) d\phi_2 = \int_0^{2\pi} q^{(2)}(\phi_2,\phi_1) d\phi_1 = 0. \tag{29}$$

This assumption is required because we cannot recover the components of the phase dynamics which are independent of the forcing phase. We will discuss this condition in more details below, after obtaining equations of the dynamics.

Let us write the transformations $\theta_{1,2} \to \phi_{1,2}$ in a form similar to Eq. (9):

$$\frac{d\phi_1}{d\theta_1} = \sigma^{(1)}(\theta_1), \quad \frac{d\phi_2}{d\theta_2} = \sigma^{(2)}(\theta_2), \tag{30}$$

with the normalization condition

$$\int_0^{2\pi} \sigma^{(1,2)}(\theta) d\theta = 2\pi. \tag{31}$$

Then Eqs. (6) can be rewritten as the equations for $\phi_{1,2}$:

$$\frac{d\phi_1}{dt} = \sigma^{(1)}(\theta_1) f^{(1)}(\theta_1,\theta_2), \quad \frac{d\phi_2}{dt} = \sigma^{(2)}(\theta_2) f^{(2)}(\theta_2,\theta_1). \tag{32}$$

Comparing the latter with Eqs. (2) we obtain

$$\omega_1 + q^{(1)}(\phi_1,\phi_2) = \sigma^{(1)}(\theta_1) f^{(1)}(\theta_1,\theta_2), \tag{33}$$

$$\omega_2 + q^{(2)}(\phi_2, \phi_1) = \sigma^{(2)}(\theta_2) f^{(2)}(\theta_2, \theta_1).$$

Integrating (33) and using the conditions (29), we finally obtain

$$\omega_1 = \frac{\sigma^{(1)}(\theta_1)}{2\pi} \int_0^{2\pi} d\phi_2 f^{(1)}(\theta_1, \theta_2), \tag{34}$$

$$\omega_2 = \frac{\sigma^{(2)}(\theta_2)}{2\pi} \int_0^{2\pi} d\phi_1 f^{(2)}(\theta_2, \theta_1). \tag{35}$$

Changing the integration variables to $\theta_{1,2}$ we obtain a closed system of equations for unknown functions $\sigma^{(1,2)}$ and constants $\omega_{1,2}$, provided the functions $f^{(1,2)}$ are given:

$$\omega_1 = \frac{\sigma^{(1)}(\theta_1)}{2\pi} \int_0^{2\pi} d\theta_2 \sigma^{(2)}(\theta_2) f^{(1)}(\theta_1, \theta_2), \tag{36}$$

$$\omega_2 = \frac{\sigma^{(2)}(\theta_2)}{2\pi} \int_0^{2\pi} d\theta_1 \sigma^{(1)}(\theta_1) f^{(2)}(\theta_1, \theta_2). \tag{37}$$

This is a nonlinear system that can be easily solved numerically (two methods are described in the Appendix). After solving this system we obtain $\omega_{1,2}$ and the transformations $\sigma^{(1)}(\theta_1)$ and $\sigma^{(2)}(\theta_2)$, which can be represented as Fourier series:

$$\sigma^{(1)}(\theta_1) = \sum_n S_n^{(1)} e^{in\theta_1}, \quad \sigma^{(2)}(\theta_2) = \sum_n S_n^{(2)} e^{in\theta_2}. \tag{38}$$

With these results we compute the phases ϕ_1 and ϕ_2 from the protophases θ_1 and θ_2 by integration of Eqs. (30):

$$\phi_1(\theta_1) = \theta_1 + \sum_{n \neq 0} \frac{S_n^{(1)}}{in} (e^{in\theta_1} - 1), \tag{39}$$

$$\phi_2(\theta_2) = \theta_2 + \sum_{n \neq 0} \frac{S_n^{(2)}}{in} (e^{in\theta_2} - 1).$$

From ϕ_1 and ϕ_2 and their derivatives, which are already given by Eqs. (32), we finally obtain by substitution the expressions for the phase dynamics:

$$\frac{d\phi_1}{dt} = q^{(1)}(\phi_1, \phi_2) = \sum_{n,m} Q_{n,m}^{(1)} e^{i(n\phi_1 + m\phi_2)}, \tag{40}$$

$$\frac{d\phi_2}{dt} = q^{(2)}(\phi_2, \phi_1) = \sum_{n,m} Q_{n,m}^{(2)} e^{i(n\phi_2 + m\phi_1)}.$$

After we have derived the equations for the phases, we would like to discuss again the assumption made at their derivation. For simplicity, we will speak about the equation for ϕ_1 only and drop for the moment the upper index. Let us represent the equation for ϕ_1 as

$$\dot{\phi}_1 = \omega_1 + q(\phi_1, \phi_2) = \omega_1 + q_0 + \tilde{q}(\phi_1) + \bar{q}(\phi_1, \phi_2), \tag{41}$$

where the separation of the term $\tilde{q}(\phi_1)$ can be made unambiguously if the condition $\int_0^{2\pi} \bar{q}(\phi_1, \phi_2) d\phi_2 = 0$ is imposed. The terms on the rhs of Eq. (41) can be interpreted as follows: ω_1 is the natural frequency, q_0 is a constant shift of this frequency due to the coupling, the term $\tilde{q}(\phi_1)$ is the coupling-induced permanent (in the sense that it does not depend on the driving phase ϕ_2) inhomogeneity of the phase rotation, and $\bar{q}$ is the part of the coupling that explicitly depends on the driving phase. In our derivation of the phases from protophases we have assumed that the term $\tilde{q}$ is not present; if it is present, we make here an approximation by neglecting it. This appears to be unavoidable: indeed, the main reason for transforming from protophases to phases is in the obtaining a maximally homogeneously rotating phase. Thus during the transformation we "cleanse" all inhomogeneities, those due to the protophases, but also those that are coupling induced, the latter being described by the term $\tilde{q}$. Since we cannot separate protophase-induced and coupling-induced inhomogeneities, we prefer to cleanse both of them.

As a result, in the obtained system (40) the term $\tilde{q}(\phi_1) = \Sigma_n Q_{n,0} e^{in\phi_1}$ is absent, as according to the construction $Q_{n,0} = 0$, if $n \neq 0$. Still, we have an uncertainty in the separation of the terms ω_1 and q_0; we discuss this problem in the next subsection.

C. Restoring natural frequencies

The constant terms in the reconstructed equations (40) are $Q_{0,0}^{(1,2)} = \omega_{1,2} + q_0^{(1,2)}$. They yield the natural frequencies only if the constant terms $q_0^{(1,2)}$ in the coupling vanish. In the examples we studied this was not the case. Nevertheless, if data sets from at least *two* observations of the same oscillators with different, though unknown, coupling strengths are available, $q_0^{(1,2)}$ can be computed under some assumptions, making the estimation of natural frequencies more precise.

We shall now discuss this issue, for simplicity, for the first oscillator only, again dropping the upper index. The main assumption is that the coupling functions for observations with different coupling strengths [we denote those by (a) and (b)] have the same form and differ by their amplitudes only. In other words, the constant terms q_0 are proportional to the norms of the phase-dependent terms:

$$\frac{q_0^{(a)}}{q_0^{(b)}} = \frac{\mathcal{N}^{(a)}}{\mathcal{N}^{(b)}}, \quad \mathcal{N}^{(a,b)} = \left(\sum{}' |Q_{n,m}^{(a,b)}|^2 \right)^{1/2}, \tag{42}$$

where the summation is over all terms except for $Q_{0,0}$. From this assumption we can easily obtain the natural frequency by making an extrapolation to the case of vanishing coupling:

$$\omega_1 = Q_{0,0}^{(b)} - \frac{Q_{0,0}^{(a)} - Q_{0,0}^{(b)}}{\mathcal{N}^{(a)} - \mathcal{N}^{(b)}} \mathcal{N}^{(b)}. \tag{43}$$

A similar equation can be written for the frequency of the second oscillator.

D. Invariance of recovered coupling functions

Finally, we demonstrate that the coupling functions, recovered with the help of Eqs. (34)–(37), are observable independent; this is valid at least for a wide class of nondegenerate observables preserving the main frequency. Suppose

that we start the reconstruction procedure with a different pair of observables $\psi_{1,2}$, related to old ones $\theta_{1,2}$, via a transformation

$$\frac{d\theta_{1,2}}{d\psi_{1,2}} = \gamma^{(1,2)}.$$

Then,

$$\frac{d\phi_{1,2}}{d\psi_{1,2}} = \frac{d\phi_{1,2}}{d\theta_{1,2}}\frac{d\theta_{1,2}}{d\psi_{1,2}} = \beta^{(1,2)},$$

with $\beta^{(1,2)}=\sigma^{(1,2)}\gamma^{(1,2)}$. Next,

$$\dot{\psi}_{1,2} = \dot{\theta}_{1,2}\frac{d\psi_{1,2}}{d\theta_{1,2}} = \frac{f^{(1,2)}}{\gamma^{(1,2)}} = g^{(1,2)}.$$

Similar to Eqs. (36) and (37) we write the equations for the transformation $\psi_{1,2}\to\phi_{1,2}$:

$$\omega_1 = \frac{\beta^{(1)}(\psi_1)}{2\pi}\int_0^{2\pi} d\psi_2 \beta^{(2)}(\psi_2) g^{(1)}(\psi_1,\psi_2),$$

$$\omega_2 = \frac{\beta^{(2)}(\psi_2)}{2\pi}\int_0^{2\pi} d\psi_1 \beta^{(1)}(\psi_1) g^{(2)}(\psi_2,\psi_1). \quad (44)$$

Substituting here $\beta^{(1,2)}$, $g^{(1,2)}$, and $d\psi_{1,2}$, one can easily see that Eqs. (44) are equivalent to Eqs. (36) and (37).

V. NUMERICAL EXAMPLES

A. Data from a phase model

As the first example, we take coupled phase oscillators—i.e., a system of coupled differential equations for phase dynamics in the form of Eqs. (2):

$$\dot{\phi}_1 = \omega_1 + \varepsilon_1 \sin(\phi_2 - \phi_1 - \beta_1),$$

$$\dot{\phi}_2 = \omega_2 + \varepsilon_2 \sin(\phi_2 - \phi_1 - \beta_2). \quad (45)$$

The parameters are $\omega_1=1$, $\omega_2=(\sqrt{5}-1)/2$, $\beta_1=\pi/4$, $\beta_2=-\pi/3$, $\varepsilon_1=0.05$, and $\varepsilon_2=0.03$. As the protophases we took *distorted* phases, calculated according to $\Theta_{1,2}=\Phi_{1,2}+\frac{1}{2}\sin(\Phi_{1,2})+\frac{1}{10}\cos(2\Phi_{1,2})$. A reconstruction of the equations of motion (6), in terms of protophases $\theta_{1,2}$, leads to the functions $f^{1,2}$, depicted in Fig. 8(a) and 8(b). Clearly, these strongly differ from the actual coupling functions in Eqs. (45). The absolute values of Fourier coefficients of the reconstructed functions $|F^{(1)}_{1,-1}|=0.050\,43$ and $|F^{(2)}_{1,-1}|=0.0302$ are very close to the true values $|F^{(1,2)}_{1,-1}|=\varepsilon_{1,2}$; however other coefficients do not vanish and are not small (e.g., $|F^{(1,2)}_{1,-2}|=0.011\,78$). Application of our method, described in Sec. IV B, provides coupling functions in terms of genuine phases $\phi_{1,2}$; these reconstructed functions are shown in Figs. 8(c) and 8(d). They are in full agreement with the rhs of the original equations (45): the absolute values of the Fourier coefficients $|Q^{(1)}_{1,-1}|=0.049\,94$ and $|Q^{(2)}_{1,-1}|=0.2994$; all other coefficients are smaller by at least two orders of the magnitude.

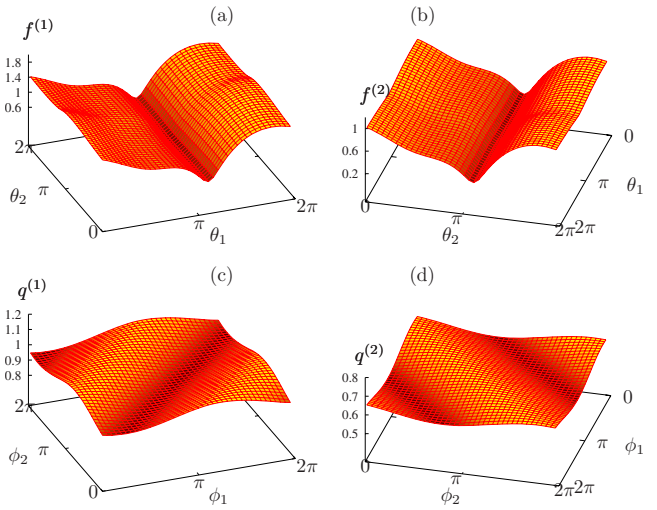

FIG. 8. (Color online) Reconstruction of phase dynamics of coupled oscillators (45) from a time series of protophases. Top panels: functions $f^{(1,2)}$ governing the dynamics of the protophases according to Eq. (6). Bottom panels: functions $q^{(1,2)}$ governing the dynamics of genuine phases, obtained from functions $f^{(1,2)}$ with the help of the transformation of Sec. IV B. These functions agree very well with the true coupling functions in the original equations (45).

B. Data from noisy van der Pol oscillators

In this subsection we test the described method using a system of two coupled noisy van der Pol oscillators

$$\ddot{x}_1 + (1-x_1^2)\dot{x}_1 + \nu_1^2 x_1 = \varepsilon(\dot{x}_2 - \dot{x}_1) + d\xi_1(t),$$

$$\ddot{x}_2 + (1-x_2^2)\dot{x}_2 + \nu_2^2 x_2 = \varepsilon(\dot{x}_1 - \dot{x}_2) + d\xi_2(t). \quad (46)$$

Here $\nu_1=1$, $\nu_2=(\sqrt{5}-1)/2$, and noise is Gaussian with correlations $\langle\xi_1(t)\xi_2(t')\rangle=\delta_{1,2}\delta(t-t')$. For this model the equations for the phases are not known analytically, so we just check the reliability of the method and its robustness toward dynamical and toward noise due to the measurement. The latter was implemented by calculating the protophases from the embedding:

$$\theta_{1,2} = \arctan\left(\frac{\dot{x}_{1,2} - 0.2 + \eta_1}{x_{1,2} - 0.2 + \eta_2}\right), \quad (47)$$

where $\eta_{1,2}$ are random variables uniformly distributed from $-d$ to d. The results for a moderate coupling $\varepsilon=0.1$ and the intensity of both noise sources $d=0.05$ are presented in Fig. 9. The upper row shows the reconstructed functions $f^{(1,2)}$ describing the dynamics in terms of the protophases $\theta_{1,2}$. One can see a strong variation of these functions with the "own" variable (i.e., $f^{(1)}$ strongly varies with θ_1, etc.). Next, we applied one-dimensional transformations to each of the protophases separately, as described in Sec. III. In these new, improved protophases $\tilde{\theta}_1$ and $\tilde{\theta}_2$ the dependence on the "own" variables is almost cleansed, as one can see from the middle row of Fig. 9. Finally, we applied the full two-dimensional transformation as described in Sec. IV to the improved protophases and obtain the final system for the genuine phases with functions presented in the bottom row of Fig. 9. One can see only a small difference between the

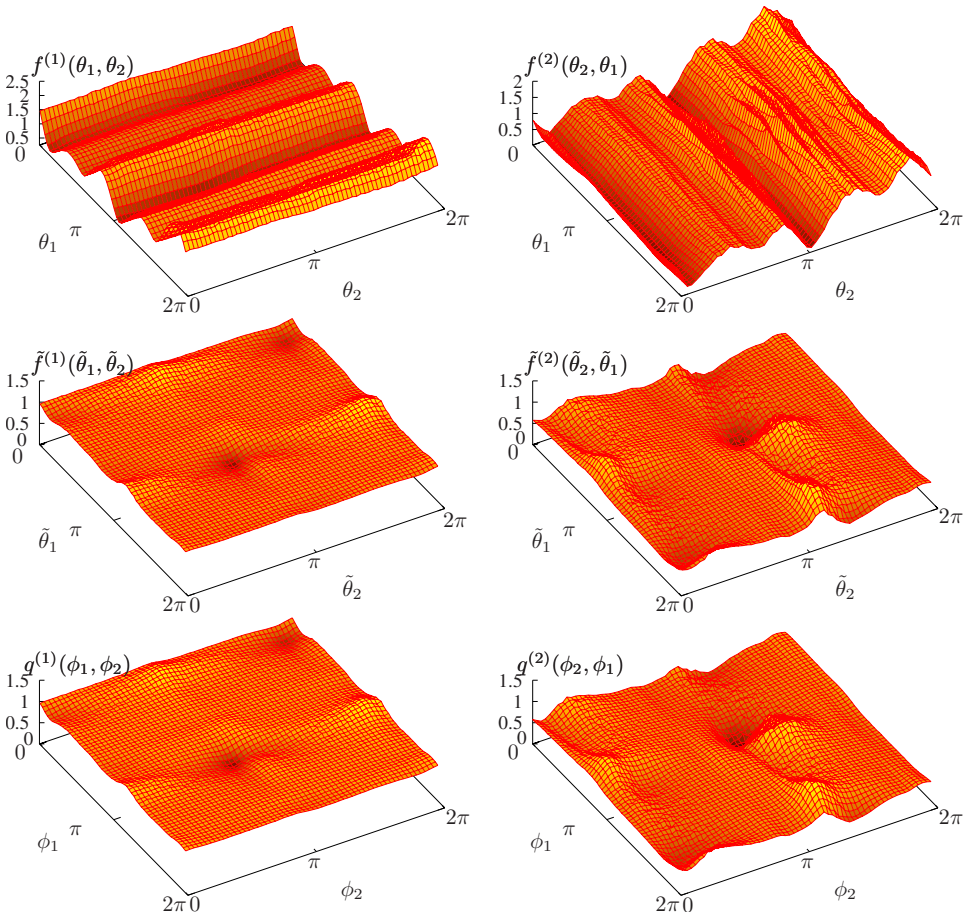

FIG. 9. (Color online) Reconstruction of the phase dynamics for coupled van der Pol oscillators with intrinsic and measuremental noises. Upper row: functions $f^{(1,2)}$ for the protophases, calculated from the embedding given by Eq. (47). Intensity of the intrinsic noise is $d=0.05$; the measuremental noise is modeled by random variables $\eta_{1,2}$, which are uniformly distributed from $-d$ to d. Middle row: functions $\tilde{f}^{(1,2)}$ for the improved protophases $\tilde{\theta}_{1,2}$ obtained by applying one-dimensional transformations to $\theta_{1,2}$. Bottom row: functions $q^{(1,2)}$ governing the dynamics of genuine phases.

improved protophases and genuine phases. Thus, in cases where a high accuracy is not needed or the data sets are rather limited, performing a one-dimensional transformation might be sufficient for practical purposes. In any case we suggest to perform such a transformation prior to the two-dimensional one, as it is rather fast and significantly reduces the computational efforts.

For a quantitative comparison of the reconstructed functions we again can compare their Fourier coefficients. We present here the results for the main interaction terms $\sim e^{i(\theta_1-\theta_2)}$ and $\sim e^{i(\phi_1-\phi_2)}$. The absolute values of the Fourier coefficients of the reconstructed functions for protophases are $|F^{(1)}_{1,-1}|=0.034\,51$ and $|F^{(2)}_{1,-1}|=0.227\,79$. After a one-dimensional transformation we obtain $|\tilde{F}^{(1)}_{1,-1}|=0.021\,30$ and $|\tilde{F}^{(2)}_{1,-1}|=0.033\,51$; the two-dimensional transformation yields $|\tilde{F}^{(1)}_{1,-1}|=0.020\,77$ and $|\tilde{F}^{(2)}_{1,-1}|=0.034\,18$. We see that for this example the coupling functions for protophases not only possess additional terms which should be eliminated, but also the amplitudes of the true modes are significantly distorted. In summary, this example again demonstrates that a transformation to true phases is a necessary step in model reconstruction.

Finally, we demonstrate the robustness of our approach with respect to noise by plotting the largest Fourier coefficients of reconstructed coupling functions versus the noise intensity. The results, shown in Fig. 10, indicate that the recovered coupling functions are rather insensitive to the noise level.

VI. PHYSICAL EXPERIMENT WITH COUPLED METRONOMES

Apart from the numerical examples above, we searched for experimental evidence supporting the efficacy of our theoretical approach. For this purpose, we performed a version of the classical Huygens experiment, examining two me-

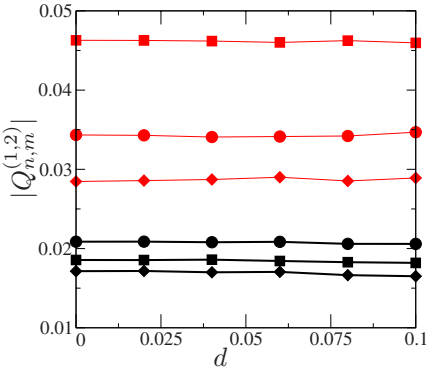

FIG. 10. (Color online) Robustness of reconstructed coupling functions $q^{(1,2)}$ with respect to noise. Absolute values of three largest Fourier coefficients $Q^{(1,2)}_{n,m}$ of $q^{(1,2)}$ are plotted against the intensity of the both intrinsic and measuremental noise d. It is seen that the variation of coefficients is rather weak. Bold black lines and solid red lines correspond to the first and second systems, respectively. Circles, squares, and diamonds represent $|Q^{(1,2)}_{1,-1}|$, $|Q^{(1,2)}_{1,1}|$, and $|Q^{(1,2)}_{3,-1}|$, respectively.

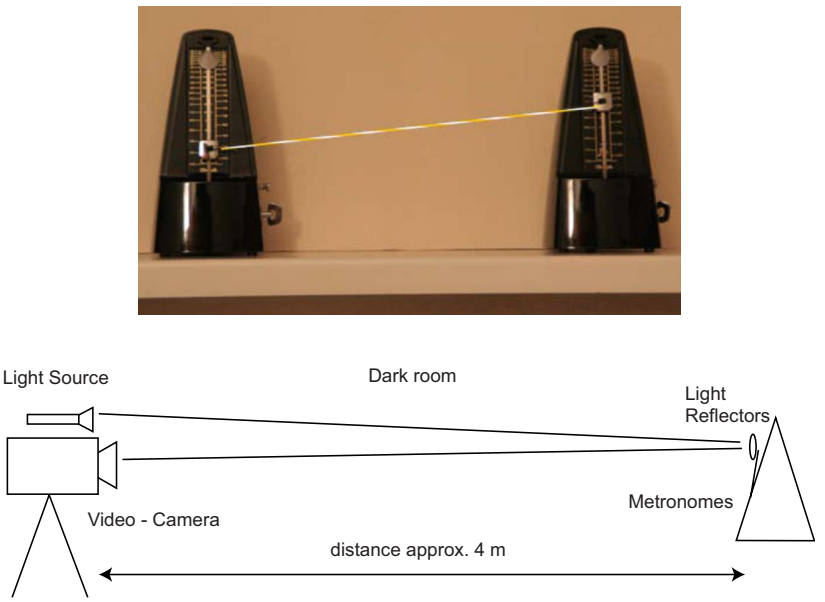

FIG. 11. (Color online) Two metronomes, placed on a rigid support (upper panel). The image of the rubber band is artificially enlarged for visibility. Scheme of the experimental setup (lower panel). The motion of the metronomes' pendulums has been filmed by a mini-DV camera for three experimental conditions: no coupling and coupling via one (as shown here) or two rubber band(s).

chanical metronomes (Cherub WSM-330), placed on a rigid base; see Fig. 11(a) (cf. [25]). The oscillation of the metronomes' pendulums was observed for three different experimental conditions: (i) metronomes are uncoupled, (ii) pendulums of the metronomes are linked by a rubber band, and (iii) pendulums of the metronomes are linked by two rubber bands.

The first measurement was used to determine the autonomous frequencies. Measurements (ii) and (iii) were used to reconstruct the coupling functions for two different coupling strengths and to recover the autonomous frequencies from observations of coupled systems by virtue of the method described in Sec. IV C. The experiment was performed twice for two different settings of autonomous frequencies.

The rubber bands were customized by longitudinal dissection to have a spring constant of about $k=0.08$ N/m; within the range of operation, k is nearly constant. The diameter of the rubber band was about 60 μm. The motion of the metronomes' pendulums was filmed by a JVC GR-D245E digital video camera (cf. [26]), with an exposure time of 1/1000 s, resolution 720×576 pixels (interlaced), and a rate of 25 frames/s, thus providing a time resolution of 0.04 s. The duration of the recording was about 140 s.

The camera was placed on a stable tripod in front of the metronomes at a distance of ≈4 m. A piece of a circular reflecting material appearing as a dot on the camera image was pasted to the top of each pendulum. The metronomes were positioned in a dark room. The reflecting material consisted of microprismatic reflecting film having the property to return the light to its source. Therefore, the light source was placed directly on the camera and directed at the metronomes in order to have the light source as close as possible to the optical system of the camera. This setup provided an excellent contrast ratio between the reflecting dots on the pendulums and the remaining structures which were effectively invisible on the captured images.

After the video capture the data was transferred to a PC via the digital fire wire interface. The movies were split into single-image frames. No blurring or any other image "enhancement" algorithm was allowed in the capturing software. The frames were de-interlaced and split vertically into two image parts, one for the left and one for the right pendulum.

A motion tracking algorithm was used for off-line processing and recovering of the horizontal and vertical coordinates of motion in time for each metronome on a frame-by-frame basis. The algorithm was implemented using the open source WXDEV-C++ development package [33]. Image processing was greatly facilitated by using the open source CIMG package [34]. The position detection algorithm uses essentially the computation of the cross-correlation function for a given frame with a picture of metronomes at rest. The shift, corresponding to a maximum of the cross correlation of each frame with the rest image, provided the position of the moving light dot.

As the scalar observable characterizing the state of metronomes, we have chosen the x coordinates of the pendulum tops of the two metronomes since the horizontal resolution of

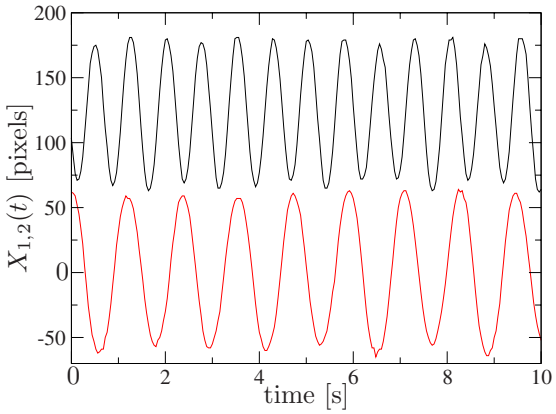

FIG. 12. (Color online) Time series of horizontal displacement for the case of metronomes, coupled via one rubber band. These signals are provided by the motion-tracking algorithm applied to video frames. Only 10 s out of ≈140 s are shown. The time series X_1 is shifted upwards for better visualization.

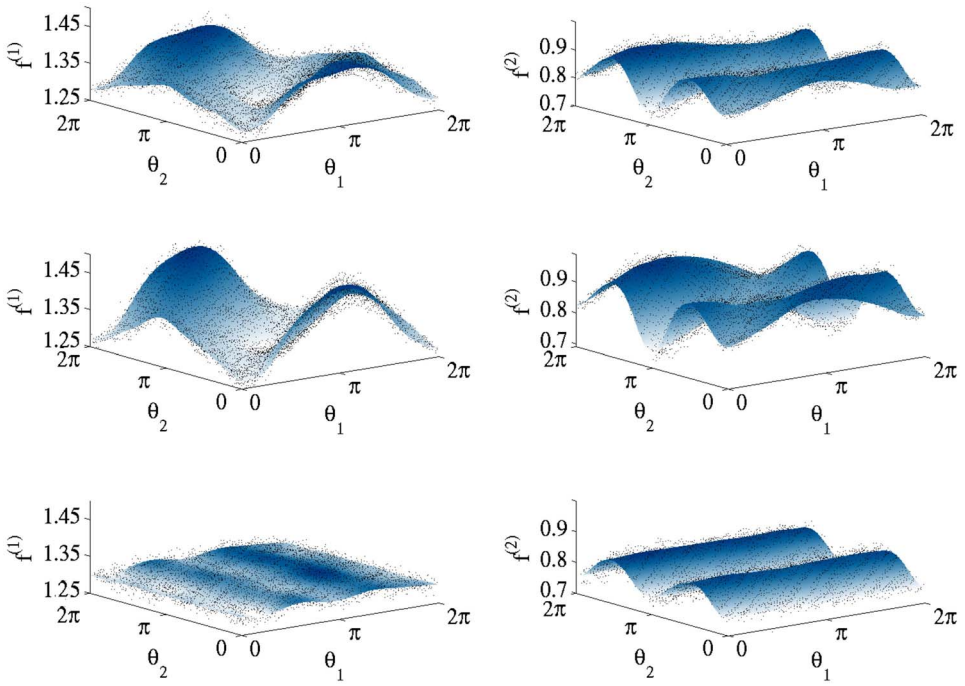

FIG. 13. (Color online) Coupling function for the protophases of metronomes. Top row: coupling with one rubber band. Middle row: coupling with two bands. Bottom row: uncoupled systems. Points show the original data; the surfaces depict the result of fitting. Notice the difference in the vertical scales of the graphs. The coupling function for the protophases of uncoupled systems does not vanish, but demonstrates a dependence on the "own" protophase.

the camera is higher than the vertical one. In Fig. 12 short segments of the time records of these observables X_1 and X_2 are presented. From these observables, the protophases were obtained by means of the Hilbert transform with a zero offset.

Next, we used our approach to reconstruct the coupling functions $f^{(1,2)}$ in terms of the protophases $\theta_{1,2}$ and to transform them to observable-independent coupling functions $q^{(1,2)}$; the results are shown in Figs. 13 and 14. Comparing the top and middle rows in Fig. 14, one can see that the coupling functions for two different interaction strengths have quite a similar form; only the amplitude is rescaled. Thus, the assumption used for the recovery of autonomous frequencies is justified. Indeed, using the analysis described in Sec. IV C, we were able to recover them with a good precision; see Fig. 15.

VII. IMPLICATIONS FOR CHARACTERIZATION OF COUPLING

Characterization of the strength, directionality, and delay in coupling from observed phases became recently a popular tool of data analysis, with applications to brain activity [9,11], cardiorespiratory interaction [7], electronic circuits [27], etc. In the following, we discuss the importance of the

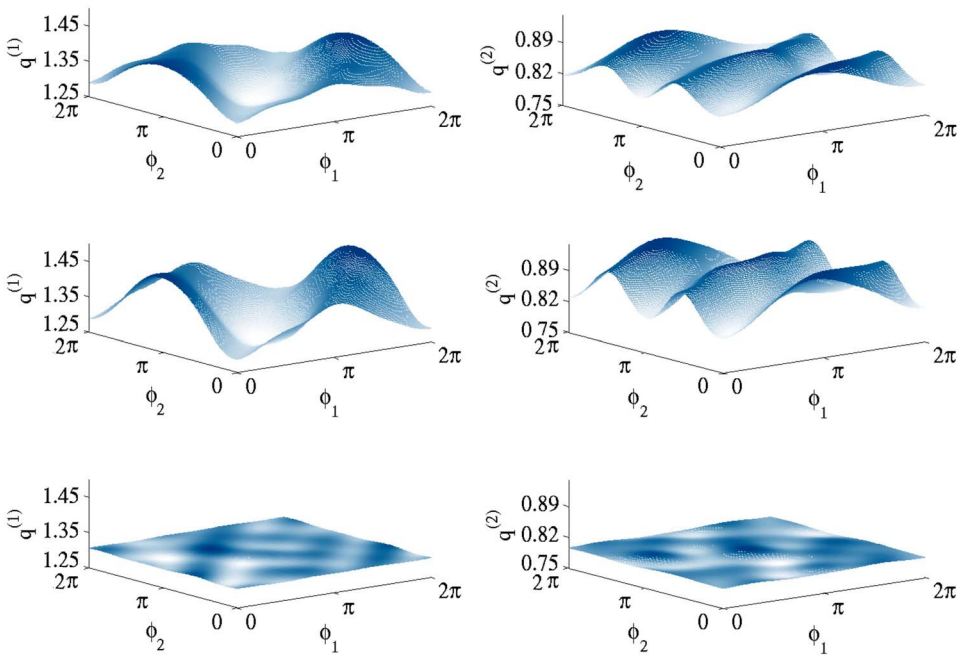

FIG. 14. (Color online) Coupling functions for the phases, obtained after application of our method to functions in Fig. 13. Top row: coupling with one rubber band. Middle row: coupling with two bands. Bottom row: uncoupled systems. The vertical scales are the same as in Fig. 13, so that one can clearly see the reduction of the phase dependence of the coupling function in the bottom row.

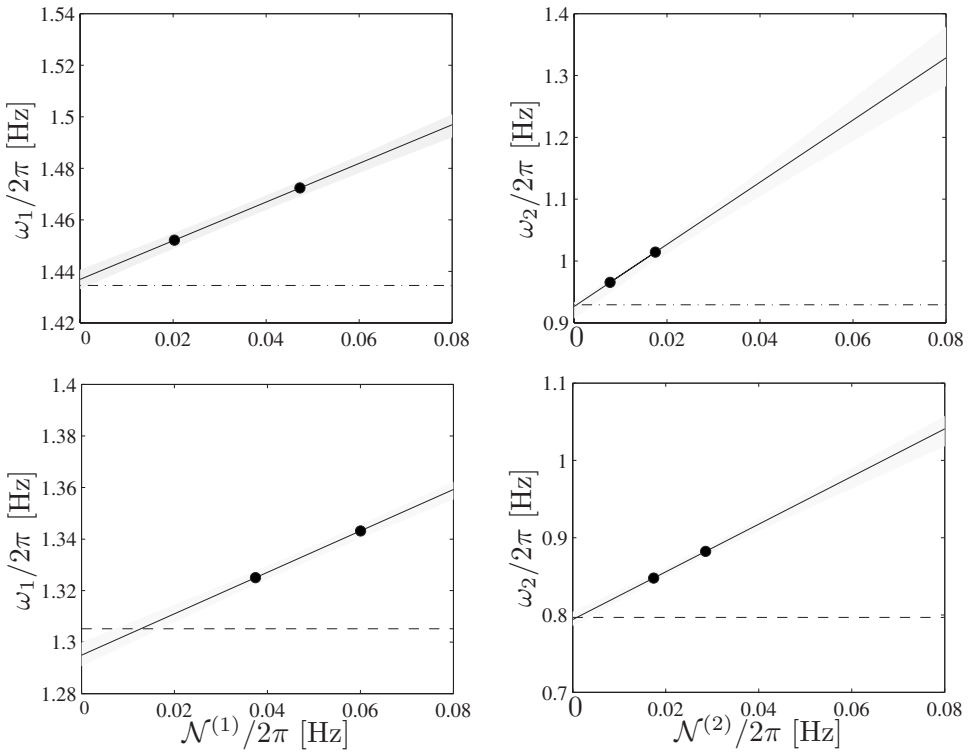

FIG. 15. Recovery of autonomous frequencies of two metronomes from observations of motion of coupled systems. Top panels, first experiment: autonomous frequencies are $\omega_1/(2\pi)=1.434$ Hz and $\omega_2/(2\pi)=0.929$ Hz. Bottom panels, second experiment: autonomous frequencies are $\omega_1/(2\pi)=1.305$ Hz and $\omega_2/(2\pi)=0.797$ Hz. Constant terms of the coupling function $\bar{\omega}_{1,2}$ are plotted vs the norm of its oscillatory component $\mathcal{N}^{(1,2)}$. The recovered natural frequencies are 1.437 ± 0.004 Hz and 0.92 ± 0.02 Hz (first setting) and 1.295 ± 0.006 Hz and 0.795 ± 0.01 Hz (second setting); they are in good agreement with the frequencies of uncoupled systems. Error bounds for linear regression, estimated from an analysis of disjoint segments of the full records, are shown as gray stripes.

above-proposed transformation $\theta\rightarrow\phi$ for the precision of this analysis.

A. Implications for the synchronization analysis

Here we consider the drastic effect, first discussed by Izhikevich and Chen [28], of the difference between the protophase and the phase on quantification of interrelation between the phases. Typically, after calculating the protophases θ_1 and θ_2 from the bivariate data, one computes the so-called "synchronization index" [29,30]

$$\gamma_{n,m}=\left|\langle e^{i(n\theta_1-m\theta_2)}\rangle\right|. \tag{48}$$

More precisely, the index $\gamma_{n,m}$ quantifies an interrelation between the protophases and cannot distinguish between synchronization and other types of interaction: e.g., modulation (see discussion in [12]). For the case of a synchronizing interaction, $\gamma_{n,m}\approx 1$ indicates $n:m$ locking.

Below, we analytically study two examples and demonstrate that the value of the synchronization index (48), computed from protophases, can be significantly biased with respect to the true value, computed from genuine phases. We emphasize that this bias is solely due to the difference between phases and protophases and not due to numerical artifacts, not discussed here.

For this goal we first suppose that the synchronization index is calculated for *independent* oscillators; certainly, in this case one expects it to vanish. However, it is easy to see that Eq. (48) yields

$$\gamma_{n,m}=\left|\langle e^{in\theta_1}\rangle\langle e^{-im\theta_2}\rangle\right|=\left|S_n^{(1)}\right|\left|S_m^{(2)}\right|, \tag{49}$$

where S_n is defined according to Eq. (14). Thus, generally, the computation of index (48) for independent oscillators from protophases provides a spurious, nonzero, value, and one obtains vanishing synchronization indices for genuine phases only, for which $S_n=\delta_{n,0}$. [An alternative approach, recently suggested by Daido [32], is to compute the synchronization index as $\gamma_{n,m}=\left|\langle(e^{in\theta_1}-\langle e^{in\theta_1}\rangle)(e^{im\theta_2}-\langle e^{im\theta_2}\rangle)^*\rangle\right|$. This measure yields correct value $\gamma_{n,m}=0$ for uncoupled oscillators.] For illustration, consider a particular relation between phases and protophases [see Eq. (30)], taking functions $\sigma^{(1,2)}=1+a_{1,2}\cos(\theta_{1,2})$, where $a_{1,2}=$const, $|a_{1,2}|<1$. Computation of the 1:1 index from protophases yields $\gamma_{1,1}=\frac{a_1a_2}{4}$; i.e., $\gamma_{1,1}$ can reach 0.25.

Consider now the other limit case, when two oscillators are perfectly 1:1 locked, so that $\phi_2-\phi_1=\alpha$, where $\alpha=$const. Computation of the synchronization index $\gamma_{1,1}$ from genuine phases certainly provides

$$\gamma_{1,1}=\left|\langle e^{i(\phi_1-\phi_2)}\rangle\right|=\left|\langle e^{-i\alpha}\rangle\right|=1.$$

Computation of the synchronization index from protophases provides

$$\gamma_{1,1} = |\langle e^{i(\theta_1-\theta_2)}\rangle| = |\langle e^{i(r_1(\phi_1)-r_2(\phi_2))}\rangle| = |\langle e^{i(r_1(\phi_1)-r_2(\phi_1+\alpha))}\rangle|,$$

where the functions $\theta_{1,2}=r_{1,2}(\phi_{1,2})$ are functions inverse to those defined by Eqs. (40). Performing the average, we write

$$\gamma_{1,1} = \left| \frac{1}{2\pi}\int_0^{2\pi} d\phi\, e^{i[r_1(\phi)-r_2(\phi+\alpha)]} \right|.$$

Considering a particular case $r_{1,2}(\phi_{1,2})=\phi_{1,2}+a_{1,2}\cos(\phi_{1,2}-\psi_{1,2})$, with constants $a_{1,2}$ and $\psi_{1,2}$, $|a_{1,2}|<1$, we obtain after integration

$$\gamma_{1,1} = |J_0[\sqrt{a_1^2+a_2^2-2a_1a_2\cos(\psi_1-\psi_2+\alpha)}]|,$$

where J_0 is the Bessel function. Its argument is smaller than 2, which implies that the spurious value of the synchronization index can be as low as 0.22—i.e., ≈4 times smaller than the true value.

To summarize this section, we emphasize that the synchronization index computed from protophases can be both over- and underestimated; this bias can be essential. The transformation from the protophases to phases prior to the calculation of the index (48) allows one to obtain the latter in a reliable and observable-independent way.

B. Implications for directionality analysis

Directionality of the coupling of two oscillators may be inferred from the reconstructed phase dynamics. Several methods of quantification and a discussion can be found in [6,16,18]. The main idea is to quantify the mutual influence of the first (second) phase on the time derivative of the second (first) one. In particular, this influence can be quantified by means of the indices

$$c_{1,2}^2 = \frac{1}{4\pi^2}\int_0^{2\pi}\int_0^{2\pi}\left(\frac{\partial q^{(1,2)}}{\partial\phi_{2,1}}\right)^2 d\phi_1 d\phi_2, \tag{50}$$

calculated from the functions $q_{1,2}$ in Eqs. (2). Furthermore, the directionality of coupling can be quantified by a single index

$$d = \frac{c_2-c_1}{c_2+c_1}, \tag{51}$$

which varies from $d=-1$, if system 2 drives system 1, and to $d=1$, if the unidirectional driving is in the other direction; the values $-1<d<1$ correspond to a bidirectional coupling.

In the case when protophases are used instead of the genuine phases, the indices $\tilde{c}_{1,2}$ are calculated in a similar way, but in terms of the reconstructed functions $f^{(1,2)}$:

$$\tilde{c}_{1,2}^2 = \frac{1}{4\pi^2}\int_0^{2\pi}\int_0^{2\pi}\left(\frac{\partial f^{(1,2)}}{\partial\theta_{2,1}}\right)^2 d\theta_1 d\theta_2. \tag{52}$$

In order to find a relation between $c_{1,2}$ and $\tilde{c}_{1,2}$, we introduce, similarly to Eqs. (30), the transformation functions $s^{(1,2)}$:

$$\frac{d\theta_1}{d\phi_1} = s^{(1)}(\phi_1), \quad \frac{d\theta_2}{d\phi_2} = s^{(2)}(\phi_2), \tag{53}$$

with an obvious relation $s^{(1,2)}(\phi_{1,2})=1/\sigma^{(1,2)}(\theta_{1,2})$. Computing the derivative of Eq. (33) we obtain

$$\frac{\partial q^{(1,2)}(\phi_1,\phi_2)}{\partial\phi_{2,1}} = \sigma^{(1,2)}(\theta_{1,2})\frac{\partial f^{(1,2)}}{\partial\theta_{2,1}}\frac{d\theta_{2,1}}{d\phi_{2,1}},$$

which yields

$$\frac{s^{(1)}(\phi_1)}{s^{(2)}(\phi_2)}\frac{\partial q^{(1,2)}(\phi_1,\phi_2)}{\partial\phi_{2,1}} = \frac{\partial f^{(1,2)}(\theta_1,\theta_2)}{\partial\theta_{2,1}}.$$

Substituting into Eq. (52) and changing integration variables, we obtain

$$\tilde{c}_{1,2}^2 = \frac{1}{4\pi^2}\int_0^{2\pi}\int_0^{2\pi}\left(\frac{\partial q^{(1,2)}}{\partial\phi_{2,1}}\right)^2 [s^{(1,2)}]^3[s^{(2,1)}]^{-1} d\phi_1 d\phi_2. \tag{54}$$

This expression differs from (50) by an observable-dependent factor $[s^{(1,2)}]^3[s^{(2,1)}]^{-1}$ in the integral. Thus, the indices calculated for protophases generally differ from those calculated for genuine phases. In the case of a unidirectional coupling, say, from system 1 to system 2, both $\frac{\partial f^{(1)}}{\partial\theta_2}$ and $\frac{\partial q^{(1)}}{\partial\phi_2}$ vanish, and, hence, the directionality can be correctly characterized both from phases and from protophases. However, in the case of a bidirectional coupling, the error due to using protophases instead of genuine phases can be highly significant.

A natural way to achieve quantification of directionality in an invariant fashion is as follows. First, we reconstruct Eqs. (2), as discussed in details above. For the given equations, the strength of the action of one system on the other is unambiguously determined by the coupling functions $q^{(1,2)}$ and can be quantified by their norms $\mathcal{N}^{(1,2)}$ [cf. Fig. 14 and Eq. (42)]. A relative dimensionless measure of this action is given by

$$C_{1,2} = \frac{\mathcal{N}^{(1,2)}}{Q_{0,0}^{(1,2)}}. \tag{55}$$

Defined in this way, the coefficients $C_{1,2}$ provide, together with Eq. (51), an observable-independent measure of directionality. Note that computation of the directionality index via Eq. (55) does not require computation of derivatives [cf. Eq. (54)], which essentially improves the numerical performance.

We emphasize, again, that here we do not bring into discussion the effects of the finite-data-size effects and noise on the estimation of indices used for quantifying the coupling characteristics (synchronization, coupling coefficients, and directionality). The effects we consider are solely due to the difference between phases and protophases and can be eliminated by the above proposed transformation.

VIII. CONCLUSION

In this paper we have described a method that bridges the gap between the theoretical description of coupled oscillatory systems and the data analysis. The key idea of the approach is to distinguish between the protophases, which are computed from scalar signals with the help of the Hilbert transform or equivalent embedding methods, and genuine phases, used in the theoretical treatment of coupled oscilla-

tors. Contrary to phases, protophases are observable dependent and nonuniversal. Therefore, an invariant description of the phase dynamics can be obtained only after a transformation from protophases to phases. We provided explicit relations for the corresponding transformation for the cases of an isolated and two interacting oscillators, and illustrated them by several numerical examples. We thoroughly discussed the reconstruction of invariant phase dynamics equations from bivariable observations of oscillatory time series. The technique we developed is applicable to weakly and moderately coupled oscillators—i.e., when the amplitudes are enslaved and the full dynamics is represented by two phases. Note that the validity of our technique goes far beyond the validity of the first-order approximation in the coupling strength used in the perturbation theory. The approach excludes the synchronous regime when the two phases become functionally related. We emphasize that our transformation from protophases to phases is not a filtering or an interpolation, but an invertible transformation that preserves all the relevant information and, at the same time, cleanses all observable-dependent features.

Furthermore we discussed the implications of our approach for characterization of the interaction from data. As first pointed out by Izhikevich and Chen [28], the synchronization index, computed without such a cleansing, can be significantly overestimated. Our results show that the estimates can be biased both upwards and downwards. After the transformation to genuine phases the calculation of the synchronization index becomes reliable. Moreover, we showed that the coupling strength and directionality can be efficiently quantified from the reconstructed equations. In this way, one significantly improves the performance of previously used approaches that exploit the dynamical equations in terms of protophases (see, e.g., [6,16–18]).

We have also shown, both theoretically and experimentally, that autonomous frequencies of self-sustained oscillators can be recovered from at least two observations of coupled dynamics if these observations correspond to different, though unknown values of coupling. Next, we have demonstrated that our techniques can be straightforwardly applied to real noisy data obtained in both physical and physiological experiments. The reconstruction of the equation for phases in the form used in the theoretical analysis significantly contributes to a better comparison of experiments and theory.

ACKNOWLEDGMENTS

We thank E. Izhikevich, H. Kantz, and E.Ott for useful discussions. We especially thank Professor J. Schaefer (IIftC Kiel) for fruitful discussions and constant support. The work has been supported by the EU (Project BRACCIA), DFG (SFB 555), and the Ursula Merz Stiftung, Berlin.

APPENDIX: SOLVING EQUATIONS FOR THE PHASE TRANSFORMATIONS

The system (34)–(37) can be solved in two different ways, described below. In the first method we employ iterations, starting, e.g., from the uniform functions $\sigma^{(1,2)}=1$. Then we calculate the frequencies $\omega_{1,2}$ from the normalization conditions

$$\frac{1}{\omega_1}=\int_0^{2\pi}\frac{d\theta_1}{\int_0^{2\pi}\sigma^{(2)}(\theta_2)f^{(1)}(\theta_1,\theta_2)d\theta_2}, \tag{A1}$$

$$\frac{1}{\omega_2}=\int_0^{2\pi}\frac{d\theta_2}{\int_0^{2\pi}\sigma^{(1)}(\theta_1)f^{(2)}(\theta_2,\theta_1)d\theta_1}.$$

Substituting this into (36) and (37), we get the next iteration for the functions σ:

$$\tilde{\sigma}^{(1)}(\theta_1)=\frac{2\pi\omega_1}{\int_0^{2\pi}\sigma^{(2)}(\theta_2)f^{(1)}(\theta_1,\theta_2)d\theta_2}, \tag{A2}$$

$$\tilde{\sigma}^{(2)}(\theta_2)=\frac{2\pi\omega_2}{\int_0^{2\pi}\sigma^{(1)}(\theta_1)f^{(2)}(\theta_2,\theta_1)d\theta_1}.$$

These iterations converge rather fast. In the practical implementation we used the functions f and σ defined on a grid.

In the second method these functions are represented via Fourier series:

$$\sigma^{(1,2)}(\theta_{1,2})=\sum_n S_n^{(1,2)}e^{in\theta_{1,2}},\quad f^{(1)}=\sum_{l,k}F_{l,k}^{(1)}e^{il\theta_1+ik\theta_2}, \tag{A3}$$

$$f^{(2)}=\sum_{l,k}F_{l,k}^{(2)}e^{il\theta_2+ik\theta_1}.$$

Substitution of these expressions into (36) and (37) yields after integration a nonlinear set of equations for unknown Fourier coefficients $S_n^{(1,2)}$:

$$\sum_{n,m}S_n^{(1)}S_m^{(2)}F_{j-n,-m}^{(1)}=\omega_1\delta_{j,0},\quad \sum_{n,m}S_n^{(2)}S_m^{(1)}F_{j-n,-m}^{(2)}=\omega_2\delta_{j,0}. \tag{A4}$$

This nonlinear system of coefficients can be solved numerically using a standard routine for finding a root of a nonlinear system, e.g., the MATLAB algorithm FSOLVE. Notice that from the normalization follows $S_0^{(1,2)}=1$.

[1] H. Kantz and T. Schreiber, *Nonlinear Time Series Analysis*, 2nd ed. (Cambridge University Press, Cambridge, England, 2004).
[2] A. M. Yacomotti, G. B, Mindlin, M. Giudici, S. Balle, S. Barland, and J. Tredicce, Phys. Rev. E **66**, 036227 (2002).
[3] M. D. Prokhorov and V. I. Ponomarenko, Phys. Rev. E **72**, 016210 (2005).
[4] I. Z. Kiss, Y. Zhai, and J. L. Hudson, Phys. Rev. Lett. **94**, 248301 (2005).
[5] J. Miyazaki and S. Kinoshita, Phys. Rev. Lett. **96**, 194101 (2006).
[6] M. G. Rosenblum, L. Cimponeriu, A. Bezerianos, A. Patzak, and R. Mrowka, Phys. Rev. E **65**, 041909 (2002).
[7] R. Mrowka, L. Cimponeriu, A. Patzak, and M. Rosenblum, Am. J. Physiol. Regulatory Integrative Comp. Physiol. **145**, R1395 (2003).
[8] R. F. Galán, G. B. Ermentrout, and N. N. Urban, Phys. Rev. Lett. **94**, 158101 (2005).
[9] L. Cimponeriu, M. Rosenblum, T. Fieseler, J. Dammers, M. Schiek, M. Majtanik, P. Morosan, A. Bezerianos, and P. A. Tass, Prog. Theor. Phys. Suppl. **150**, 22 (2003).
[10] J. Gross, L. Timmermann, J. Kujala, M. Dirks, F. Schmitz, R. Salmelin, and A. Schnitzler, Proc. Natl. Acad. Sci. U.S.A. **99**, 2299 (2002).
[11] A. Schnitzler and J. Gross, Nat. Rev. Neurosci. **6**, 285 (2005).
[12] A. Pikovsky, M. Rosenblum, and J. Kurths, *Synchronization. A Universal Concept in Nonlinear Sciences* (Cambridge University Press, Cambridge, England, 2001).
[13] E. Rodriguez, N. George, J.-P. Lachaux, J. Martinerie, B. Renault, and F. J. Varela, Nature (London) **397**, 430 (1999).
[14] D J. DeShazer, R. Breban, E. Ott, and R. Roy, Phys. Rev. Lett. **87**, 044101 (2001).
[15] H. Daido, Physica D **91**, 24 (1996).
[16] M. G. Rosenblum and A. S. Pikovsky, Phys. Rev. E **64**, 045202(R) (2001).
[17] L. Cimponeriu, M. G. Rosenblum, and A. S. Pikovsky, Phys. Rev. E **70**, 046213 (2004).
[18] M. G. Rosenblum, L. Cimponeriu, and A. S. Pikovsky, in *Handbook of Time Series Analysis*, edited by J. Timmer, B. Schelter, and M. Winterhalder (Wiley-VCH, Weinheim, 2006), pp. 159–180.
[19] I. T. Tokuda, S. Jain, I. Z. Kiss, and J. L. Hudson, Phys. Rev. Lett. **99**, 064101 (2007).
[20] B. Kralemann, L. Cimponeriu, M. Rosenblum, A. Pikovsky, and R. Mrowka, Phys. Rev. E **76**, 055201(R) (2007).
[21] Y. Kuramoto, *Chemical Oscillations, Waves and Turbulence* (Springer, Berlin, 1984).
[22] D. Gabor, J. Inst. Electr. Eng., Part 1 **93**, 429 (1946).
[23] B. Kralemann, L. Cimponeriu, M. Rosenblum, and A. Pikovsky (unpublished).
[24] A. L. Goldberger, L. A. N. Amaral, L. Glass, J. M. Hausdorff, P. C. Ivanov, R. G. Mark, J. E. Mietus, G. B. Moody, C.-K. Peng, and H. E. Stanley, Circulation **101**, e215 (2000),circulation electronic pages: http://circ.ahajournals.org/cgi/content/full/101/23/e215
[25] J. Pantaleone, Am. J. Phys. **70**, 992 (2002).
[26] T. Greczylo and E. Debowska, Eur. J. Phys. **23**, 441 (2002).
[27] B. P. Bezruchko, V. Ponomarenko, A. S. Pikovsky, and M. G. Rosenblum, Chaos **13**, 179 (2003).
[28] E. M. Izhikevich and Y. Chen (unpublished).
[29] F. Mormann, K. Lehnertz, P. David, and C. E. Elger, Physica D **144**, 358 (2000).
[30] M. G. Rosenblum, A. S. Pikovsky, J. Kurths, C. Schäfer, and P. A. Tass, in *Neuro-informatics and Neural Modeling*, edited by F. Moss and S. Gielen, Vol. 4 of Handbook of Biological Physics (Elsevier, Amsterdam, 2001), pp. 279–321.
[31] R. Quian Quiroga, A. Kraskov, T. Kreuz, and P. Grassberger, Phys. Rev. E **65**, 041903 (2002).
[32] H. Daido (unpublished).
[33] See http://wxdsgn.sourceforge.net/.
[34] See http://cimg.sourceforge.net/.